Journal of Cluster Science (2024) 35:519–532
https://doi.org/10.1007/s10876-023-02491-y

ORIGINAL PAPER

Curcumin Loaded onto Folic acid Carbon dots as a Potent drug Delivery System for Antibacterial and Anticancer Applications

Eman Serag[1] · Mohamed Helal[1] · Ahmed El Nemr[1]

Received: 13 May 2023 / Accepted: 11 August 2023 / Published online: 11 September 2023

Abstract

Numerous malignancies have been shown to be successfully treated with Curcumin. Despite its promising effects, Curcumin has limitations in clinical studies because of its stability, low water solubility, and adsorption. Carbon quantum dots with high biocompatibility can be employed as nanostructured material carriers to enhance Curcumin availability. In this study, folic acid was used as the raw material for the hydrothermal preparation of carbon dots, followed by the loading of Curcumin onto the carbon dots to form a folic acid carbon dot/Curcumin nanocomposite. The morphology and the chemical structure of the synthesized carbon dots were investigated. Folic acid carbon dots displayed robust emission peaks with a quantum yield of 41.8%. Moreover, the adsorption effectiveness of Curcumin on carbon dots was determined to be 83.11%. The liberating pattern of Curcumin was pH-dependent and reached 36 and 27% after a few hours at pH 5 and 7.4, respectively. The release occurs via the Fickiann diffusion mechanism with ah *n* value less than 0.45. The nanocomposite was tested for antibacterial activity against gram-negative *Pseudomonas aeruginosa ATCC 27,853* and gram-positive *Staphylococcus aureus ATCC 25,923*. The nanocomposite displayed antibacterial behavior with MIC 12.5 µg/mL. The anticancer activities of the nanocomposite were further tested against high-folate receptor-expressing Hela cells (cervical malignancy) and low-folate receptor-expressing HepG2 cells (hepatocellular carcinoma). Folic acid carbon dot/Curcumin nanocomposite reduced Hela cell viability at an IC_{50} of 88.723 ± 0.534 g/mL. On the other hand, HepG2 cells showed no toxicity response.

Highlights

- Hydrothermal preparation of carbon dots (CDs) using folic acid as a Curcumin loading.
- The synthesis of amorphous carbon dots had an average particle size of 6.8 ± 2.1 nm.
- CDs loaded with Curcumin are active against gram-positive and gram-negative bacteria.
- Anticancer properties of CDs against a high folate receptor-expressing Hela cells.
- The anticancer properties of CDs against a low folate receptor-expressing HepG2.

Keywords Carbon dots · Folic acid · Curcumin · Cervical cancer · Hepatocellular carcinoma

Introduction

Curcumin [1,7-bis(4-hydroxy-3-methoxyphenyl)-1,6-heptadiene-3,5-dione] is a naturally occurring polyphenolic compound extracted from the Asian plant *Curcuma longa* (turmeric) [1] with several biological properties [2, 3] such as anti-inflammatory [4, 5], anti-oxidant [6], antidiabetic [7], anti-microbial [8, 9] and anti-cancer [10, 11]. Although Curcumin exhibited intriguing biological features, its low solubility, poor bioavailability, fast biotransformation, and degradability limit its widespread biological applications [12]. Diverse techniques, including structural chemical

✉ Ahmed El Nemr
ahmedmoustafaelnemr@yahoo.com;
ahmed.m.elnemr@gmail.com

Eman Serag
d.emanserag@yahoo.com

Mohamed Helal
m.helalf@gmail.com

[1] National Institute of Oceanography and Fisheries (NIOF), Kayet Bey, Elanfoushy, Alexandria, Egypt

modification, dispersion on a variety of polymeric matrices, and lipid addition increased the biological threshold of Curcumin [13]. However, a significant proportion of generated derivatives exhibited minimal biological activity [14, 15].

Innovative Nanotechnology for Drug Delivery can increase Curcumin's bioavailability and tumor cell-targeting. Upon surface adsorption, nanoparticles' chemical and physical characteristics can improve the Curcumin hydrophilicity [16]. Among different nanoparticle categories, CDs are a promising class of photoluminescent carbon nanomaterials with a spherical shape and a size < 10 nm [17]. They are highly hydrophilic, have low toxicity, and are biocompatible. In comparison to other classic fluorescent materials, such as quantum dots (QDs), their photoluminescent capabilities are the most attractive. This has led to their widespread usage in biological and environmental analyses, and they also play a significant role in bioimaging and medication targeting [18–20]. Yang and coworkers created a pH-sensitive nano-drug carrier based on cyclodextrin coated with carbon dots to transport doxorubicin into Hela and HEK293T cells. In vivo, loading cinobufagin onto liposomes conjugated with near-infrared CDs enhances the anticancer efficacy and minimizes dose-related adverse effects.

Carbon dots can be produced using various biomolecules and biopolymers used as "precursors". Folic acid (FA) is a key cellular binding ligand for optimal cell survival and tissue homeostasis [21]. FA has a high level of biocompatibility and affinity for various epithelial cells. FA is a low molecular weight vitamin that binds to its specific folate receptor (FR) in which it is known to be highly upregulated in cancerous tumors of epithelial origin [22] such as breast [23], liver [24], ovarian [25, 26] and lung [27]. In comparison to normal cells, tumor cells express FR at a considerably higher level. They also have a significant affinity for fatty acids, which are essential for accelerated metabolism and growth (DNA synthesis and methylation) [28]. Therefore, tumor cells with varying levels of FR expression respond well to FA as a binding ligand. FA or folate complexes enter the cell via receptor-mediated endocytosis upon attaching to the tumor cell surface membrane without producing an immunogenic response [29, 30]. Utilizing FA carriers guarantees a highly focused delivery of drugs to tumor cells.

In this work, folic acid carbon dots (FACDs) were produced hydrothermally from the folic acid precursor. Curcumin was loaded onto FACDs to create Curcumin-folic acid carbon dots (Cur-FACDs), characterized in structure and pH-dependent release kinetics. Cur-FACDs' antibacterial effect was also studied using gram-positive *Staphylococcus aureus ATCC 25,923 (S. aureus*) bacteria and Gram-negative *Pseudomonas aeruginosa ATCC 27,853* (*P. aeruginosa*) bacteria. Cur-FACDs were examined for their anticancer activity against highly tumorigenic and metastatic cervical cancer cell lines (Hela cells) and liver cancer cells (HepG2).

Materials and Methods

Materials

Alpha Chemika, India, provided the folic acid (98%). Curcumin (94% curcuminoid content) and quinine sulphate were provided by Sigma-Aldrich, USA. Ethanol (C_2H_5OH, 94–96%) was provided by Merck (Germany). Gram-negative *Pseudomonas aeruginosa ATCC 27,853 (P. aeruginosa)* and gram-positive *Staphylococcus aureus ATCC 25,923* (*S. aureus*) bacteria were obtained from Ain shams university subjected to antibacterial tests. Hela cells (for cervical cancer) and HepG2 cells (for hepatocellular carcinoma) and fibroblast normal cells were purchased from Nawah Scientific Inc. for use in cell line tests (Mokatam, Cairo, Egypt). Cells were kept alive at 37 °C in a humidified, 5% v/v CO_2 environment using RPMI medium improved with 100 mg/mL streptomycin, 100 units/mL penicillin, and 10% heat-inactivated foetal bovine serum.

Methods

Synthesis of Carbon dots Based on Folic acid (FACDs)

Folic acid-carbon dots (FACDs) were produced using hydrothermal synthesis as follows: After dispersing 0.1 g of folic acid in 50 mL deionized water with sonication for 30 min, the mixture was heated at 200 °C for 5 h in a Teflon-lined autoclave cup. To remove macroparticles, the brownish solution was centrifuged at 10,000 rpm for 30 min. Finally, the obtained FACDs were stored at 4 °C before further analyses and applications [31].

Calculation of FACD Quantum Yield

The quantum yield (Q_y) of the synthesized FACD was obtained via comparing its fluorescence to that of the standard sample quinine sulphate (Q_y=0.54) [31]. Quinine sulphate was dissolved in 0.1 mol/L H_2SO_4. The FACDs were dissolved in deionized water prior to synthesis and Quantum yield (Qy) of FACDs is calculated considering the following Eq. 1:

$$Qy_{(FAD)} = Qy_{(standard)} \frac{(FA\eta^2)_{FACD}}{(FA\eta^2)_{Standard}} \quad (1)$$

where $Q_{y(FACD)}$ represents the quantum yield of the synthesized FACD, $Q_{y(standard)}$ represents the quantum yield of

quinine sulphate as a standard the integrated emission intensity is represented as F, A is the UV-vis spectrophotometer absorbance at the excitation wavelength, and η is the solvent refractive index (1.33 for H_2SO_4, and deionized water).

Characterization of FACDs

Synthesized FACDs were categorized using UV-visible absorption spectra, Fourier transform infrared (FTIR), and transmission electron microscopy (TEM). The sample was diluted in deionized water for UV measurements, which were conducted at room temperature using a HITACHI U-3900 UV/visible spectrophotometer (Japan) with an absorption wavelength range of 200 to 800 nm. Fluorescence spectra were obtained using an F-2700 fluorescence spectrophotometer (Hitachi High Technologies, Japan) with a quartz cuvette measuring 0.5 cm in diameter.

The morphological features and particle size of sample were investigated with The TEM images. FACDs were analyzed on a JEOL 2100 PLUS (Japan) with an accelerating voltage of 100 kV. The sample was diluted in water and sonicated for 15 min. After that, 20 µL of sample was deposited onto formvar carbon film on 300 mesh copper grid and air-dried at room temperature. The FTIR analysis was accomplished in the spectral range of 400–4000 cm^{-1} and at a spectral resolution of 4 cm^{-1} at room temperature on a Bruker Vertex 70 FTIR spectrometer linked to a Platinum ATR model V-100, Germany. The FACDs' sample was diluted by deionized water for examination of zeta potential by a Zetasizer Nano ZS90 (Malvern Instruments, Manchester, UK).

Curcumin Loading on FACDs

The folic acid carbon dots (FACDs) surface was loaded with Curcumin (Cur) as follows: FACDs were mixed with Curcumin in ethanol in a 2:1 ratio. The reaction mixture was shaken at 200 rpm in a dark for 24 h at room temperature. FACD loaded with Cur was obtained by removing unreacted Curcumin from the supernatant after 15 min of centrifugation at 10,000 rpm. Then dried under vacuum overnight. The adsorption efficiency of Curcumin on FACDs concerning the total amount of cur loaded was obtained by a UV/vis spectrophotometer at 425 nm, and calculated using Eq. (2).

$$Adsorptionefficiency\% = \frac{Totalamountof Cur - freeamountof Cur}{Totalamountof Cur} \times 100 \quad (2)$$

2.2.5 Curcumin Release Kinetics

FACDS-Cur (5 mL) was placed in a dialysis bag with 100 mL phosphate buffer (PBS) and shaken at 200 rpm to evaluate the Curcumin release efficiency from FACDs-Cur at different pH media (5 and 7.4). Samples were taken out of the dialysis bag at regular times and replaced with the same amount of PBS. The Curcumin amount released was calculated by a UV-spectrophotometer and plotted against the calibration curve [32]. The Eq. (3) was used to calculate the release %:

$$CumulativeRelease\% = \frac{Curcuminreleased}{CurcumininFACDs} \times 100 \quad (3)$$

To explain the drug release mechanism, the zero order, first order, and krosmeyer-peppa models were utilized to calculate the releasing profile of Curcumin [33, 34]. Zero-order Eq. (4):

$$Q_{t=}Q_0 + K_0 t \quad (4)$$

where Q_t is the dose dissolved in time t, Q_0 is the dose at the start of the experiment, and K_0 is the zero-order release constant (expressed as a concentration per unit time).

First-order Eq. (5):

$$LogQ_t = LogQ_{0-}K_t/2.303 \quad (5)$$

where Q_0 is the drug concentration at the beginning and K is a constant of first order.

Korsmeyer and Peppas Eq. (6):

$$Log\left(M_T/M_\infty\right) = logk + nLogt \quad (6)$$

where M_T and M_∞ are the fractions of the drug released at time t and infinite time, respectively, k is a kinetic constant, and n is the release exponent, which indicates how the drug is transported.

Anti-bacterial Activity of FACDs and Cur-FACDs

FACDs and Cur-FACDs antimicrobial activity was determined by agar well diffusion assay [35]. Gram-negative bacteria, *Pseudomonas aeruginosa (ATCC 27,853)* and Gram-positive bacteria, *Staphylococcus aureus (ATCC25923)* were used for this assay. At 37 °C, nutrient broth medium was used to cultivate bacterial strains. Then, 50 g/mL of each material (FACD and FACD - Cur) was evaluated against *Pseudomonas aeruginosa (ATCC 27,853)* and *Staphylococcus aureus (ATCC25923)*. The zone of inhibition was then calculated based on the inhibition zone diameter (well diameter) of each compound surrounding each well (in millimetres). In all treatments, the experiment

was conducted using three repetitions, and the resulting mean values were reported.

Minimum Inhibitory Concentration (MIC) Evaluation

The minimum FACD and FACD-Cur concentrations required to inhibit *Pseudomonas aeruginosa* and *Staphylococcus aureus* development were established. The antimicrobial test was initiated with 50 µg/mL initial concentrations of FACD and FACD-Cur. Following the process of serial dilutions in saline solution and subsequent plating on nutrient agar, an inoculum volume of 100 µL containing 1108 colony-forming units per millilitre (cfu/mL) was introduced onto an agar medium and poured onto a Petri plate. The Petri plate was then incubated for a period of one night. To serve as a positive control, ampicillin, a pharmaceutical agent employed in the treatment of infections, was assessed in conjunction with FACD and FACD-Cur samples. The MIC values were determined in triplicate using the microplate serial dilution technique, and the mean values were reported.

Anti-cancer Activity of FACDs and Curcumin Loaded FACDs

MTT Assay for Normal Cells Availability To assess cell viability, the formula shown below was utilized. Using the MTT (3-(4,5-dimethylthiazol-2-yl)-2,5-diphenyltetrazolium bromide) test, cell viability following treatment with FACD and FACD-Cur was assessed. Recapitulating the procedure, a 96-well plate was seeded with a fibroblast cell suspension (50 µL) at a density of 3×10^3 cells/well and then incubated for 24 h at 37 °C with 5% CO_2. The cells were subsequently exposed to 100 µL of either FACD-Cur or FACD at doses of 10, 20, 40, 60, 80, and 100 µg/mL. As a reference point for comparison, the untreated cells in the culture media were used. The MTT solution (100 µL, 0.5 mg/mL) was added to each well after 72 h of incubation at 37 °C in the dark. The crystals of formed formazan were dissolved in 100 µL of DMSO. A microplate reader was used to measure the absorbance at λ_{max} 570 nm three times during the experiment. To assess cell viability, the Eq. (6) shown below was utilized [36].

$$Cellavalibility\% = \frac{OD_{Treated}}{OD_{Control}} \tag{7}$$

Sulforhodamine B (SRB) Assay for Anticancer Activity Detection Cell viability against examined substances was evaluated using the Sulforhodamine B (SRB) assay [37]. 5×10^3 cells were seeded in 100 µL aliquots of cell suspension, which were then plated in 96-well dishes and cultured for 24 h in a CO_2 incubator with full medium. For 72 h, cells were exposed to media aliquots (100 µL) containing drugs at various concentrations (10, 20, 40, 60, 80, and 100 µg/mL). The cells were then fixed in 150 µL of 10% trichloroacetic acid (TCA) and left to rest at 4 °C for an hour after the medium supernatant was removed. After discarding the TCA solution, the cells were washed with distilled water five times. It was then incubated for 10 min at room temperature in the dark after the addition of the SRB solution (0.4% w/v). It was then washed three times with 1% CH_3CO_2H and air dried for an entire night. Finally, TRIS (10 mM) was added to dissolve the protein-bound SRB stain, and absorbance at λ_{max} 540 nm was measured using a microplate reader from Ortenberg, Germany, equipped with a BMGLABTECH®-FLUO star Omega. At least three times, each experimental group received at least four sets of data.

Statistical Analysis The findings of all tests were combined to compute the average and standard error of the mean. The data were analysed using Minitab 16 software with a significance level of $p<0.05$ using one-way analysis of variance (ANOVA).

Results and Discussion

Characterization of the Synthesized FACDs

Carbon dots can be synthesized using a variety of techniques, including microwave heating, pyrolysis, sonication, heating, chemical reactions, and laser ablation [38]. Here, we used the hydrothermal fabrication method because it is simple, low-cost, non-toxic, and environmentally friendly. Carbon precursors (FA) are placed in a sealed Teflon-equipped stainless steel autoclave with water to synthesize carbon dots under high temperature and pressure [39]. To further investigate the nanostructures of the produced FACDs, their morphology and particle size distribution were examined using high-resolution TEM. The surface morphology and average diameter distribution of the produced FACDs were analyzed using TEM (Fig. 1a, b). Carbon dots formed from folic acid were amorphous and had an average particle size of 6.8 ± 2.1 nm.

To further understand the optical characteristics of the created FACDs, the UV-vis absorption and fluorescence spectra were acquired. FACD contains two peaks at λ 250 and 288 nm, with a shoulder at λ 326 nm, as shown in Fig. 2a. These peaks, which correspond to the $\pi \underset{\rightarrow}{\ } \pi^*$ electron transition and $n \underset{\rightarrow}{\ } \pi^*$ electron transition, respectively, are

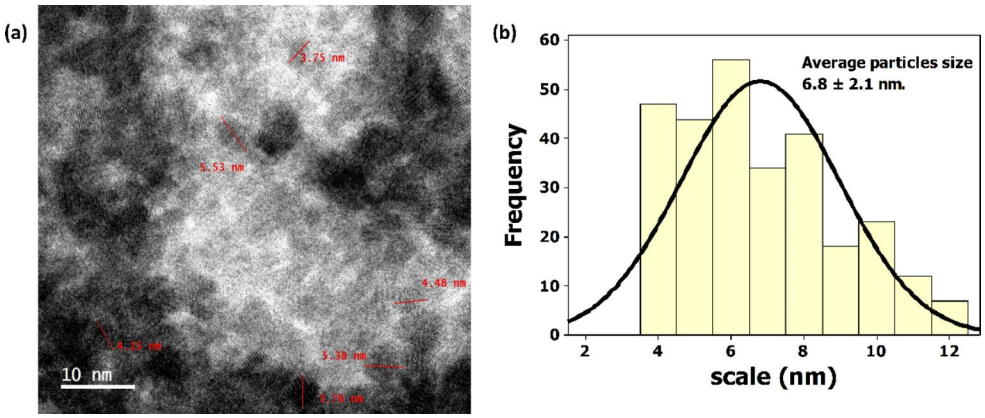

Fig. 1 (a) Morphology of FACDs, (b) Particle size distribution obtained from the TEM image

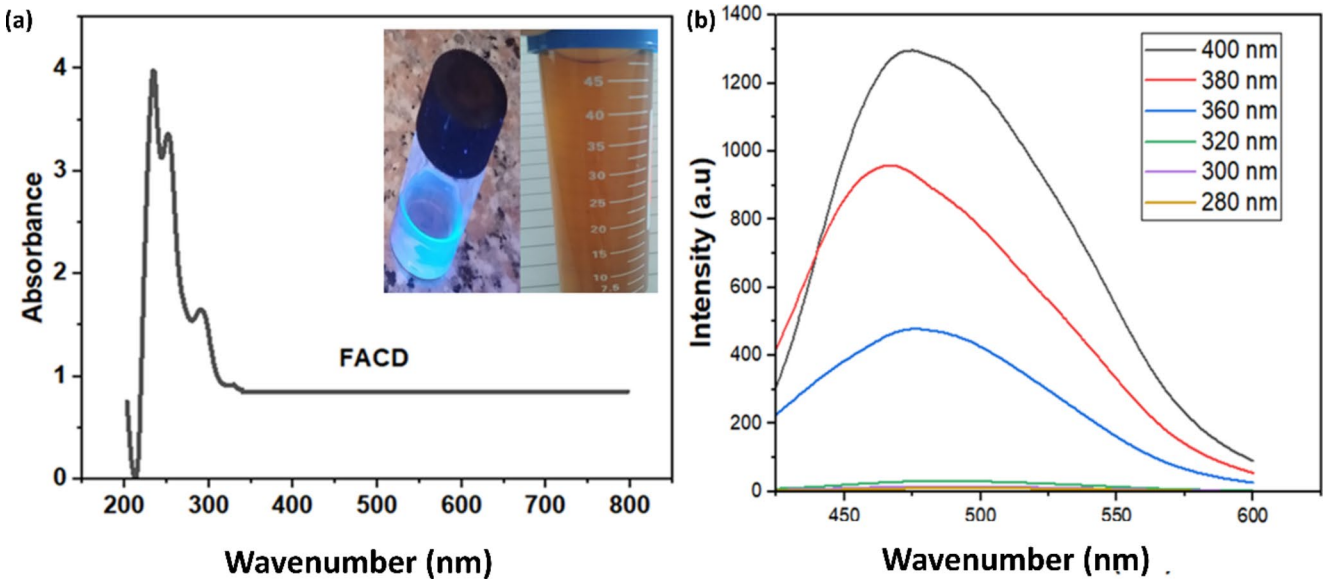

Fig. 2 (a) UV – vis absorption spectra of FACDs, and the inset represents the photographic image of FACD under visible light on the right and at λ_{max} 365 nm UV light on the left (b) Excitation dependent fluorescence spectra of FACDs

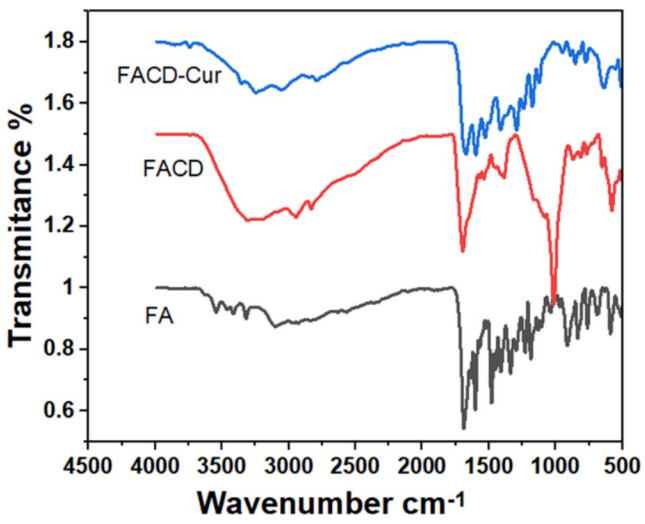

Fig. 3 FTIR spectrum of FA, and FACDs.

visible on the spectrum [40]. Excitation-dependent behavior at various excitation wavelengths reveals the presence of the emission peaks (Fig. 2b). FACDs displayed significant emission peaks, which were caused by the formation of conjugate-domains (carbon core) in the CDs structure [41, 42]. The Q_y of the synthesized FACDs reached 41.8%, using quinine sulphate (0.1 mol L^{-1} H_2SO_4 solution) as a reference with a quantum yield of 54%, contributed. This result is comparable to that of previous studies [31, 43]. The FACDs are brown in the daytime and generate a brilliant blue fluorescence when λ_{max} 365 nm UV light excites them (inset of Fig. 2a).

FTIR spectra for folic acid (FA) and the synthesized FACDs are displayed in Fig. 3. In the folic acid spectra, the adsorption bands at 3358 and 3076 cm^{-1} are related to stretching vibrations of O–H and C–H, respectively. While the adsorption band at 1693 cm1 represents the carbonyl group (C = O) of carboxylic acid [44]. FACD's FTIR

spectrum includes the same functional groups as FA: the stretching vibrations of O-H, C-H, C = O, and C-N at 3322, 2941, 1693, and 1020 cm^{-1}, respectively [45, 46].

Curcumin Loading on FACDs and Kinetic Release

Curcumin's poor solubility as a chemotherapeutic agent is a key concern for its use in biomedical applications. Curcumin is mostly soluble in organic solvents including ethanol, DMF, and DMSO and is only weakly soluble in water [47]. Therefore, the challenge of obtaining Curcumin solution stability can be avoided by placing Curcumin onto nanomaterial carriers.

To determine the stability of Curcumin loading on FACDs, a zeta potential analysis was performed. As depicted in Fig. 4a,b, FACDs zeta potential at pH 7 was − 17.4 mV, which was in good agreement with previous results that interpreted the negative zeta potential as the presence of ionized carboxylic groups of FA [48]. Cur-FACDs experienced a positive shift in their zeta potential to -11.5 mV. The observed phenomenon can be explained by the electrostatic attraction forces between folic acid conjugated dendrimers (FACDs) and Curcumin, as well as the hydrogen bonds formed between the amine groups of folic acid and the ketones and hydroxyl groups of Curcumin. These

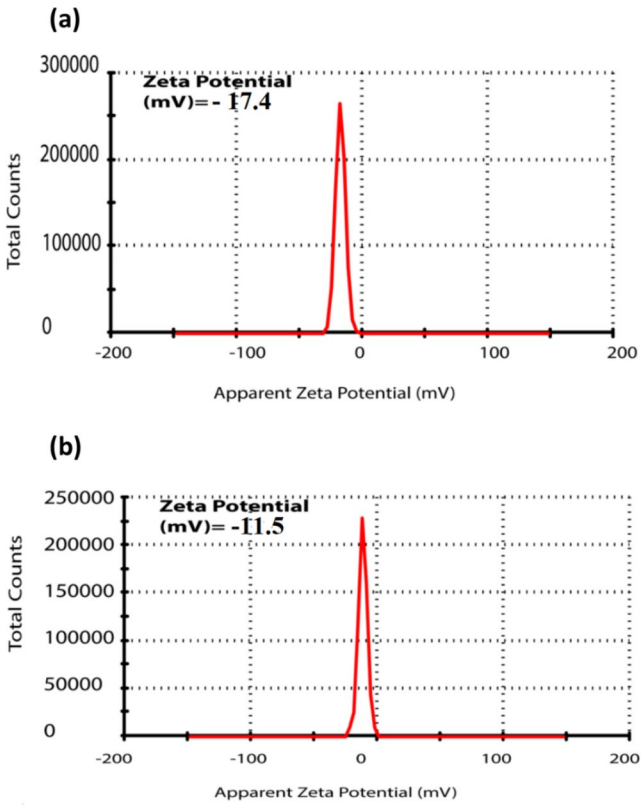

Fig. 4 Zeta potential of (a) the synthesized folic acid carbon dots (FACDs), (b) Curcumin loading on folic acid carbon dots (FACDs-Cur).

interactions result in a change in the zeta potential and an increase in the particle size of FACD from 6.2 ± 1.3 nm to 73.2 ± 2.4 nm upon loading Curcumin. This change in particle size serves as evidence for the successful loading of Curcumin [3, 49, 50]. Furthermore, FACDs-cur spectra in Fig. 3. Supports the conjugation of Curcumin with FACDs via H-bonds and electrostatic attraction. Curcumin's OH-related stretching at 3500 cm^{-1}, its C = O vibration exhibit at 1624 cm^{-1}, and its C-O enol group stretching at 1275 cm^{-1} were all observed [51, 52].

The adsorption efficiency of Curcumin on FACDs surface was measured to be 83 ± 1.5%, demonstrating a significant electrostatic interaction between Curcumin and FACDs. The basis for Curcumin entrapment is the interaction of Curcumin's keto-form with FACDs through weak supramolecular type bonds and electrostatic interactions. The low aggregation and amorphous structure of FACDs enhanced drug endocytosis in the overexpressed folate receptor cancer cells [3, 53]. Due to their excellent encapsulation, release efficiencies, and great biocompatibility, these FACDs loaded with Curcumin were determined to be the ideal framework technique for hydrophobic drug delivery [54]. The pattern of Curcumin release over 80 h was depicted in Fig. 5 at mildly acidic pH 5 and neutral pH 7.4. However, the loading of Curcumin is found to be pH dependent because of the functional groups surface manipulation. The percentage of Curcumin released was higher at pH 5 than at pH 7.4, which is likely due to the effect of acidic medium on carboxylic functional group protonation, resulting in a weak electrostatic interaction between Curcumin and FACDs [55]. Results from an FTIR study of FACD and FACD-Cur indicate that this is a significant constituent. However, Curcumin was gradually released at both pH levels, with the initial Curcumin percentages reaching 36 and 27% after a few hours, respectively. The sustained release has a significant advantage in that it keeps the desired concentration of drug in the plasma while avoiding undesirable side effects, reducing dose frequency, and enhancing patient comfort [56].

The behavior of curcumin release was studied using the zero order, first order, and Kosmeyer and Peppas models. As presented in Fig. 6 and according to Table 1, the release of curcumin was best fitted to Kosmeyer and Peppas models, which exhibit R^2 values of 0.94 and 0.948 at pH 5 and pH 7.4, respectively. This is because carbon dots have a polymeric-like structure [57]. In addition, the exponent of diffusion (n) values at pH 5 and 7.4 were 0.255, 0.336 and less than 0.45, indicating that Curcumin is released by the Fickian diffusion mechanism [58]. Chen and colleagues also investigated the Curcumin release behavior on PLGA/chitosan fibers in vitro and found that the release mechanism follows the Fickian diffusion mechanism [58]. Furthermore,

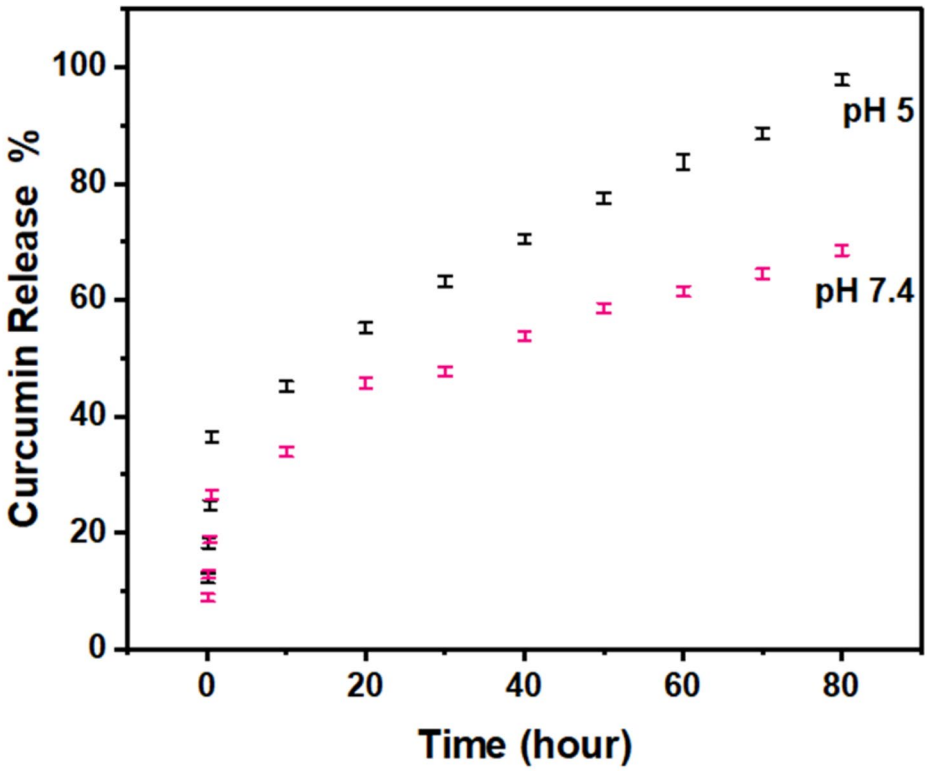

Fig. 5 The pattern of Curcumin release at pH 5, and pH 7.4 (data are expressed as standard error of mean)

Curcumin loading on silk Fibroin nanoparticles followed the Korsmeyer Peppas model with n values less than 0.45 [59]. Additionally, Curcumin loaded on carbon nanodots (E-CNDs and U-CNDs) followed a controlled sustained pattern, releasing 60 and 74% of the Curcumin at 72 h, respectively, at pH 5 [3].

The in vitro Cytotoxicity Effect of FACD and FACD-Cur

MTT Assay

Systemic toxicity, multidrug resistance, and nonspecific interaction are major problems with current chemotherapeutic regimens [60]. The use of a soluble, biodegradable, and selectively targeted cancer cell drug delivery system (DDS) is preferable because it can reduce these unfavorable side effects [61].

An intensive research input has been put to utilize Folic acid carbon dots, a specific delivery system for cancers with high folate receptors [62, 63]. FA is small in size (441-Da) with stability over different temperature and pH ranges. Also it is non-immunogenic with high binding affinity to its respective receptor [64]. FA is a strong binding ligand for its respective α and β receptors. Preparing of folic acid carbon dot nanoparticles introduce FA as a promising drug delivery system for highly expression folate receptor tumors [65]. Folate receptor (FR) comprise two forms α and β that are anchored on cell surface via glycosyl-phosphatidyleinositol (GPI) anchor [66]. Most normal cells lack both receptor expression except specific epithelial cells that express FR-α without blood circulation accessibility [67]. On the other hand, FR-α is overexpressed in various tumors such as ovarian [68], cervical [69] and non-small cell lung carcinoma [70]. FR-β is predominantly linked to hematopoietic cancers [71].

MTT assay was used to test FACD and FACD-Cur for non-cytotoxicity and safety against normal fibroblast normal cell lines. As presented in Fig. 7a, the vitality of the cell lines remains greater than 95% at high concentrations of both FACD and FACD-Cur (100 µg/mL), indicating that no cytotoxicity is observed for FACD as a drug delivery approach.

The findings of this study are comparable to those reported in reference [72], where the effects of quercetin/curcuminoid mixtures at concentrations ranging from 5 to 25 µg/mL were examined on a human dermal fibroblast cell line. The results showed that the cell viability exceeded 80% after 24, 48, and 72 h of exposure. Furthermore, a study by [36] examined the MTT assay of graphene quantum dots (GQDs) conjugated with glucosamine (GlcN). The findings of this study indicated that the unmodified nanocarrier exhibited no

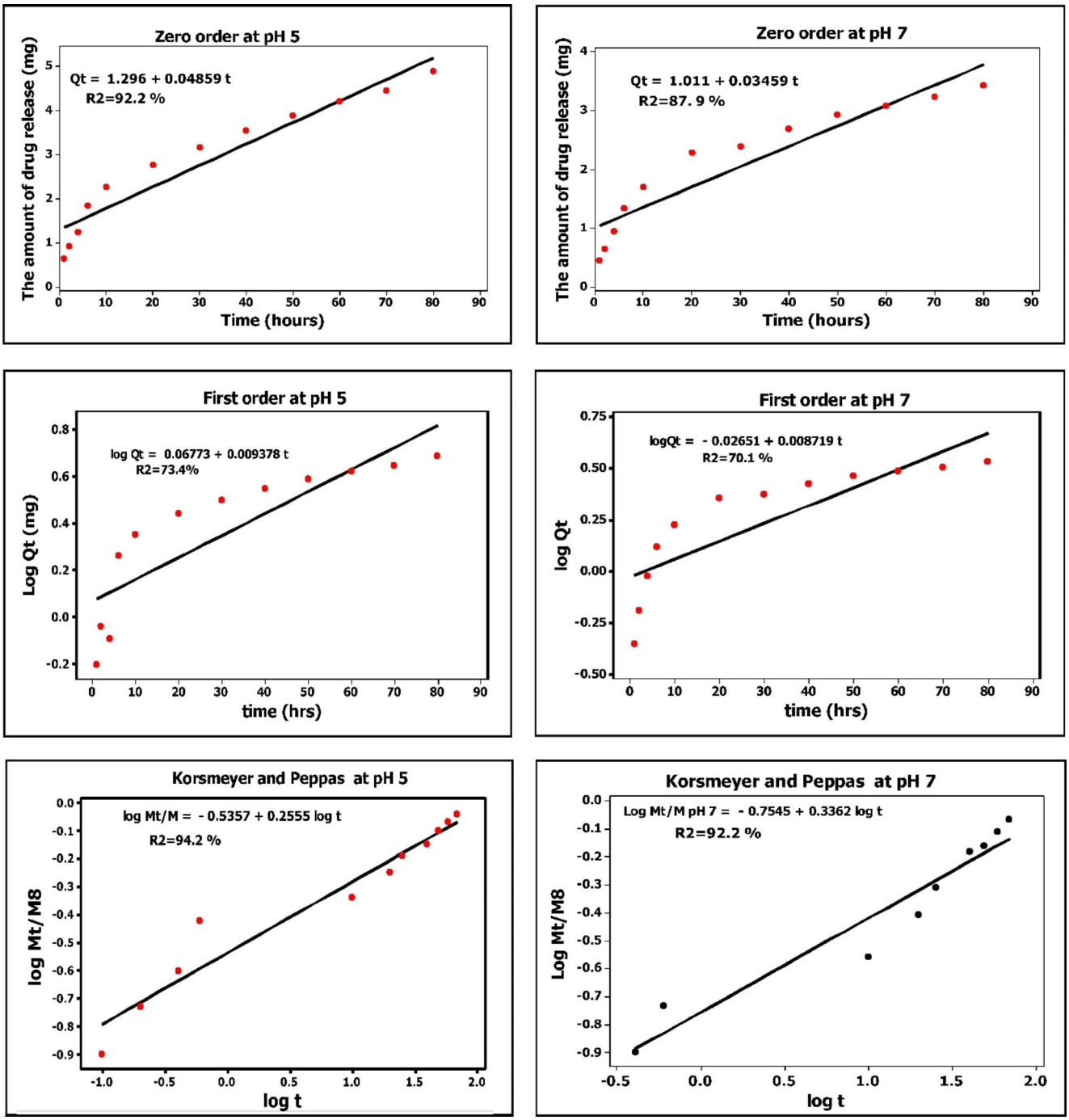

Fig. 6 Drug release profile of FACD-Cur at pH 5, and pH 7.4 with zero, first order, and Korsmeyer-Peppas models

Table 1 The kinetic parameters of curcumin release mathematical models

Mathematical models	Zero order R^2	First order R^2	Korsmeyer Peppas R^2
pH 5	92.2	73.3	94.2, n = 0.255
pH 7	87.9	70.1	92.2, n = 0.336

toxicity, as evidenced by a cell viability rate exceeding 94% even at concentrations as high as 50 $\mu g \cdot ml^{-1}$.

SRB Assay

As shown in Fig. 7b, high doses of Cur-FACDs (100 µg/mL) caused toxicity in cells with a lot of folate receptors, like Hela cells. This effect couldn't be seen in HepG2 cells

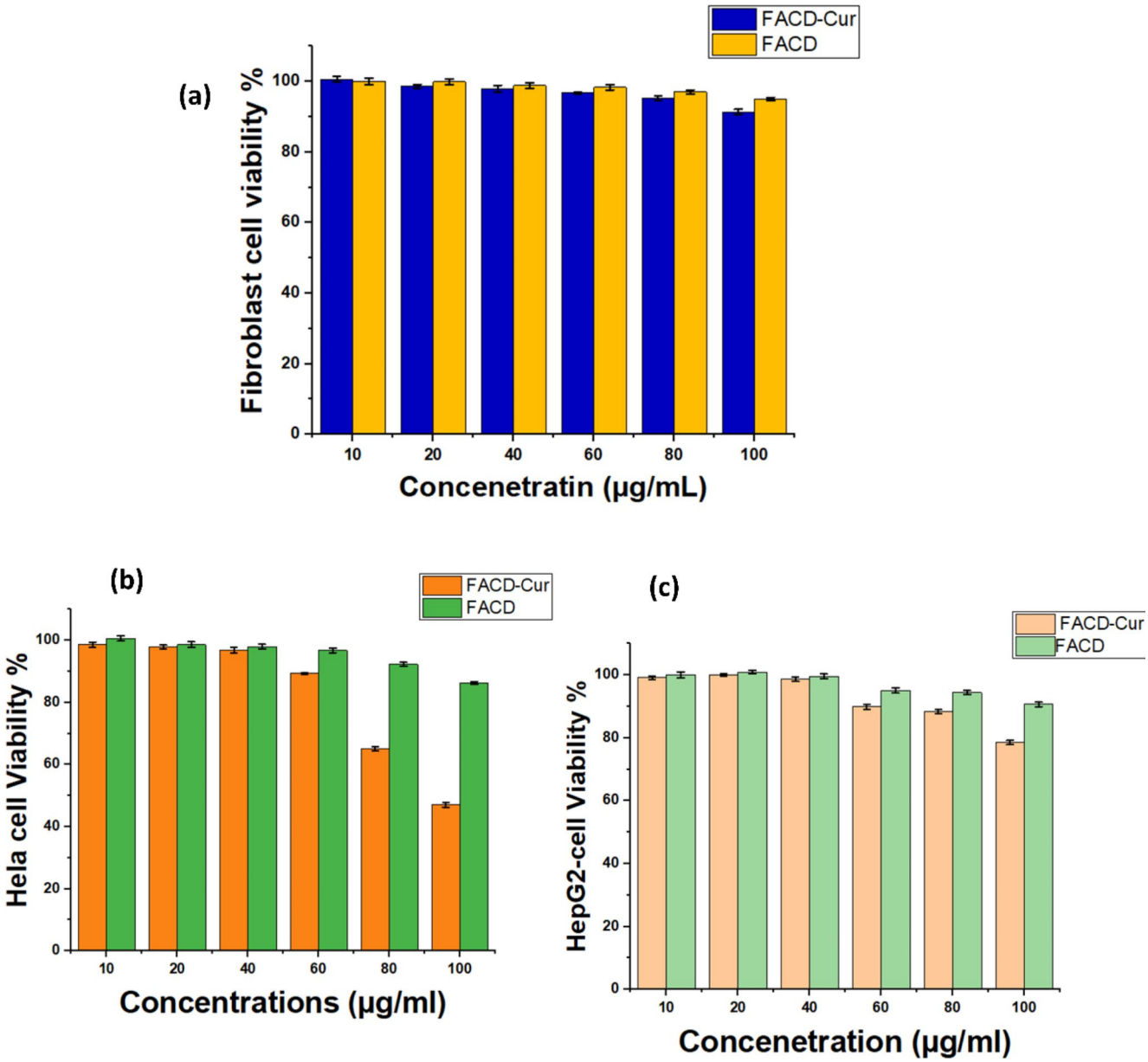

Fig. 7 (a) MTT assay for FACD and FACD-Cur on fibroblast normal cells. (b and c) Anticancer activity of FACD and FACD-Cur on Hela and HepG2 cells as determined by the SRB assay. For 72 h, the cells were exposed to various concentrations (10, 20, 40, 60, 80, and 100 µg/mL). The data were presented as means ± SD (n = 3)

or other cells with low levels of folate receptors (Fig. 7c). Folic acid carbon dots loaded with Curcumin (FACDs-Cur) reduced Hela cell viability at IC50 of 88.723 ± 0.534 µg/mL. On the other hand, HepG2 cells did not show any toxicity response. This can be clarified by the fact that Hela cells have more folic acid receptors than fibroblast cells, and HepG2, as a targeting ligand, increases cellular uptake of its attached drug via receptor-mediated endocytosis [73, 74].

In previous studies, Folate nano dots have been used as a delivery system to efficiency deliver unsymmetrical Bisacridines to treat lung and prostate cancer cells [75]. Otherwise, cytotoxic drug Etoposide loaded on FACDs led to significant growth inhibition of Hela cells [76].

A possible explanation of Curcumin anticancer activity is derived from that Curcumin induced DNA damage in Hela cells through nuclei fragmentation and chromatin condensation [77]. Low dose Curcumin decreases cell proliferation and viability through DNA hypermethylation and decreasing nuclear organizer region-associated proteins AgNOR levels [78] or inhibit their proliferation via the NF-kB and Wnt/β pathways inhibition leading to G2/M cell cycle arrest [79]. In addition, Hela cells treated with Curcumin exhibit

dysregulated thioredoxin system and elevated levels of ROS [80]. Furthermore, Curcumin and its phytochemical derivatives were found to induce Hela cell metabolic reprograming by modulating lactate-pyruvate metabolism and inhibit their metastasis [81].

Curcumin has been shown to have a significant inhibitory effect on the NF-kB factor, which is responsible for the expression of numerous proteins such as cytokines and interferons, which induce inflammation and cancer disease progression [82]. Furthermore, Curcumin inhibited the production of the transcription factor AP-1, which has an anti-apoptotic effect in most cancer types [83]. Another study found that Curcumin had anti-cancer activities in malignant mesothelioma through regulating IL-1 and NFkB factors [84]. Curcumin, on the other hand, inhibited the expression of IL-6, TLR, IL-3, and STAT-1 in human chronic myelogenous leukemia cells (K562) [85].

In this research, the FACD synthesized from precursor folic acid via hydrothermal process is a promising drug carrier system to target tumors with high folate receptor expression. FACD-Cur was highly toxic to Hela cells at concentrations significantly lower than those previously reported in the literature [86]. That has the potential to boost FACD's use as a targeted cancer drug delivery system.

FACDs Anti-bacterial Activity

Recent work reported that the Curcumin antibacterial activity against several bacterial species, including MSSA and MRSA [87]. Here in our study, we have shown that Curcumin loaded on folic acid carbon dots exhibit potent antibacterial activity against *S. aureus* and *P. aeruginosa* at a concentration as low as 12.5 µg/mL with MIC of 25% (Fig. 8, and Table 2). Curcumin's antibacterial effect may be mediated via the generation of reactive oxygen species, which leads to the destruction of bacterial cell membranes and cell death. Furthermore, FACD-mediated Curcumin administration improves its solubility, promotes Curcumin targeting, and increases bioavailability [88].

Our results demonstrated that FACD, when used as a nano-carrier system for Curcumin, significantly improved the antibacterial activity of Curcumin, resulting in a minimum inhibitory concentration (MIC), which was much lower than that reported for the other systems. Previous research has tested Curcumin's efficacy against ten different *S. aureus* strains (including MSSA and MRSA reference strains) at concentrations ranging from 125 to 250 µg/mL [89].

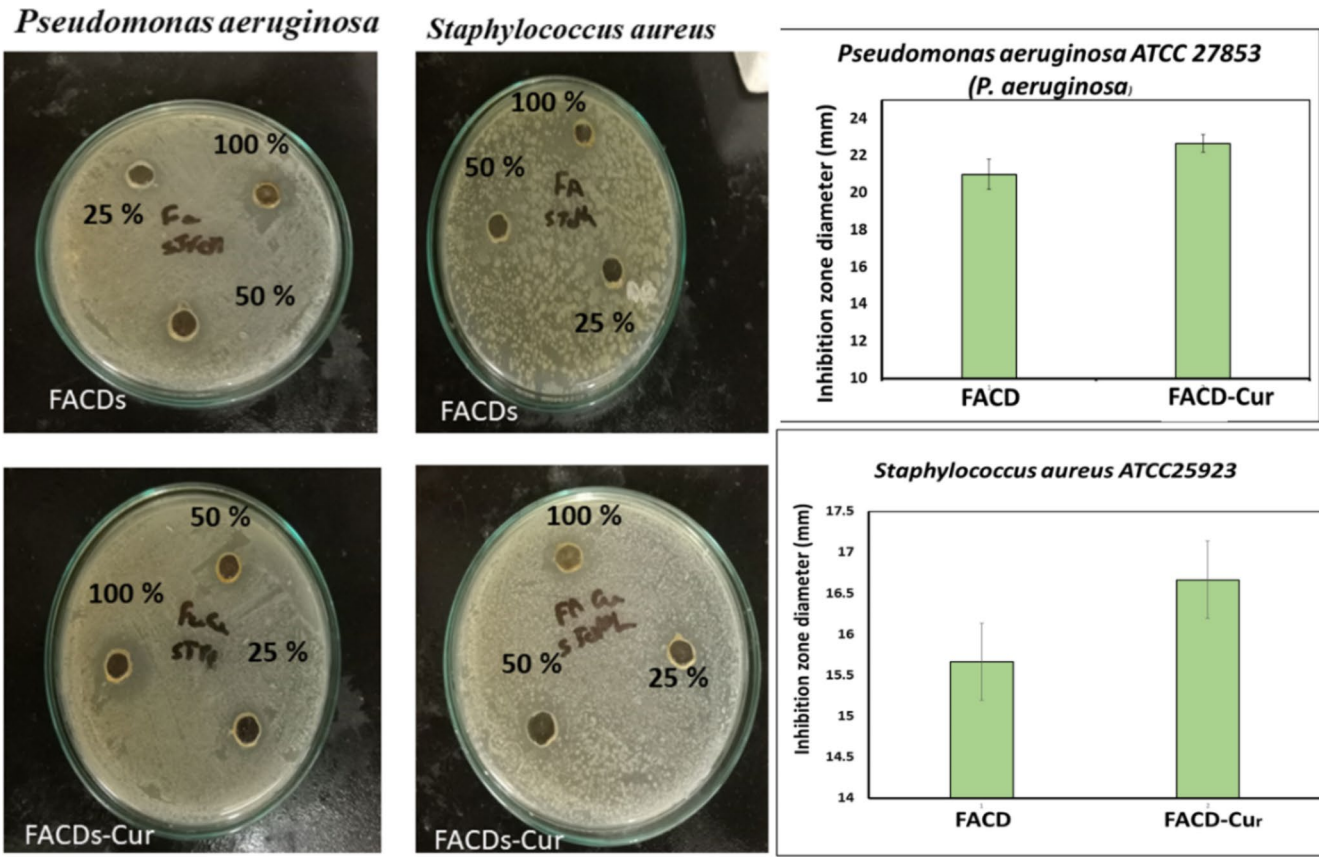

Fig. 8 Antibacterial activity of FACDs, and FACDs-Cur against *Pseudomonas aeruginosa ATCC 27,853 (P. aeruginosa)* and *Staphylococcus aureus ATCC 25,923 (S. aureus)*. Data are presented as means ± SD ($n = 3$, *$p < 0.05$)

Table 2 Minimum inhibition concentration of FACDs, and FACDs-Cur against *Pseudomonas aeruginosa ATCC 27,853 (P. aeruginosa)* and *Staphylococcus aureus ATCC 25,923 (S. aureus)*

Pathogenic strain	Inhibition zone diameter (mm)**			MIC
Sample Concentration	100%	50%	25%	
Gram negative bacteria				
Pseudomonas aeruginosa ATCC 27,853				
FACDs	20 ± 0.445	19 ± 0.345	14 ± 0.471	12.5 µg/mL
FACDs-Cur	23 ± 0.435	15 ± 0.475	13 ± 0.521	12.5 µg/mL
Antibiotic (0.1%)	38 ± 0.231			
Gram positive bacteria				
Staphylococcus aureus ATCC25923				
FACDs	15 ± 0.521	10 ± 0.486	ND	25 µg/mL
FACDs-Cur	17 ± 0.547	15 ± 0.643	13 ± 0.442	12.5 µg/mL
Antibiotic (0.1%)	30 ± 0.447			

In another study, Curcumin that had been changed chemically and was called Curcumin-1 (CUR-1) was tested against *S. aureus*. The MIC concentration was found to be 18.42 µg/mL [90]. The same compound was effective against *S. aureus* at MIC 250 µg/mL, according to a study by Sasidharan et al. [91]. Also, the growth of *S. aureus* was stopped by the Curcumin analogue indium Curcumin at a MIC of 187.5 µg/mL [91]. Antibacterial activity of Curcumin nanoparticles (2–40 nm in size) was demonstrated against *S. aureus* (MIC of 150 and 100 µg/mL for DMSO and water dissolved particles, respectively) and *P. aeruginosa* (MIC of 250 and 200 µg/mL for DMSO and water dissolved particles, respectively) [92]. Copper-oxide Curcumin nanocomposite showed antibacterial activity against *S. aureus* and other bacterial species [93]. The minimum inhibitory concentration (MIC) for Curcumin against *S. aureus* and *P. aeruginosa* was found to be between 25 and 512 µg/mL [94]. Curcumin and its gallium-Curcumin nanoparticles had MIC values of 41.37 and 82.75 µg/ml against bacteria, respectively [95]. Curcumin's median inhibitory concentration (MIC) against *S. aureus* reference and clinically isolated strains was found to be 250 µg/mL and 5000 µg/mL, respectively, in another study [8]. Curcumin and iron oxide nanocomposites coated with sodium alginate were also synthesized in another study. They found that the minimum inhibitory concentration (MIC) of Curcumin alone against *S. aureus* and *P. aeruginosa* is 31.25 and 125 µg/mL, respectively. The minimum inhibitory concentration (MIC) of nanocomposite against *S. aureus* and *P. aeruginosa*, respectively, was 15.62 and 62.5 µg/mL, while the MIC of nanocomposite without Curcumin was 875 µg/mL [96].

Conclusion

CDs were successfully generated from folic acid by a low-cost hydrothermal synthesis. The synthesized FACDs were successfully and efficiently loaded with Curcumin. Since curcumin's release was pH-dependent, tumor cells, which have low pH levels, received more of the substance when it was released at pH 5 as opposed to normal cells. FACDs-Cur has demonstrated antibacterial activity against gram-negative bacteria (*Pseudomonas aeruginosa ATCC 27,853* and gram-positive bacteria (*Staphylococcus aureus ATCC 25,923*). Curcumin and FACDs were further conjugated to increase the desired anticancer properties for Hela cells. In summary, FACD is an efficient and precise nano-delivery system, and when loaded with Curcumin, the combined system showed promising anti-cancer and anti-bacterial properties.

Author Contributions Dr. E. Serag carried out the experimental work and wrote the original manuscript. Dr. M. Helal conducting a portion of the experimental work and participating in the data analysis and original text writing. Prof. A. El Nemr Financial support of the work, supervision of the experimental work, writing, reviewing, and editing the final manuscript, and submission to journal. All authors have read and given their consent to the final, published version of the manuscript.

Funding Not applicable.
Open access funding provided by The Science, Technology & Innovation Funding Authority (STDF) in cooperation with The Egyptian Knowledge Bank (EKB).

Data Availability The datasets used and/or analyzed during the current study are available from the corresponding author on reasonable request.

Declarations

Competing Interests The authors declare no competing interests.

Ethics Approval and Consent to Participate Not applicable.

Consent for Publication Not applicable.

References

1. M. T. Kabir, M. H. Rahman, R. Akter, T. Behl, D. Kaushik, V. Mittal, P. Pandey, M. F. Akhtar, A. Saleem, G. M. Albadrani, M. Kamel, S. A. M. Khalifa, H. R. El-Seedi, M. M. Abdel-Daim.Biomolecules. 11(3), (2021). https://doi.org/10.3390/biom11030392
2. M. Urošević, L. Nikolić, I. Gajić, V. Nikolić, A. Dinić, V. Miljković.Antibiotics. 11(2), 135 (2022).
3. D. M. Arvapalli, A. T. Sheardy, K. Allado, H. Chevva, Z. Yin, J. Wei.ACS Appl Bio Mater. 3(12), 8776–8785 (2020). https://doi.org/10.1021/acsabm.0c01144
4. S. Fuloria, J. Mehta, A. Chandel, M. Sekar, N. N. I. M. Rani, M. Y. Begum, V. Subramaniyan, K. Chidambaram, L. Thangavelu, R. Nordin, Y. S. Wu, K. V. Sathasivam, P. T. Lum, D. U. Meenakshi, V. Kumarasamy, A. K. Azad, N. K. Fuloria.Frontiers in Pharmacology. 13, (2022). https://doi.org/10.3389/fphar.2022.820806
5. M. Zhang, X. Zhang, T. Tian, Q. Zhang, Y. Wen, J. Zhu, D. Xiao, W. Cui, Y. Lin.Bioactive Materials. 8, 368–380 (2022). https://doi.org/10.1016/j.bioactmat.2021.06.003
6. N. Aftab, A. Vieira.Phytotherapy research: PTR. 24(4), 500–502 (2010). https://doi.org/10.1002/ptr.2960
7. L. T. Marton, L. M. Pescinini-e-Salzedas, M. E. C. Camargo, S. M. Barbalho, J. F. d. S. Haber, R. V. Sinatora, C. R. P. Detregiachi, R. J. S. Girio, D. V. Buchaim, P. Cincotto dos Santos Bueno. Frontiers in Endocrinology. 12, (2021). https://doi.org/10.3389/fendo.2021.669448
8. A. Adamczak, M. Ożarowski, T. M. Karpiński.Pharmaceuticals (Basel, Switzerland). 13(7), 153 (2020). https://doi.org/10.3390/ph13070153
9. H. Gunes, D. Gulen, R. Mutlu, A. Gumus, T. Tas, A. E. Topkaya.Toxicol Ind Health. 32(2), 246–250 (2016). https://doi.org/10.1177/0748233713498458
10. K. Mansouri, S. Rasoulpoor, A. Daneshkhah, S. Abolfathi, N. Salari, M. Mohammadi, S. Rasoulpoor, S. Shabani.BMC Cancer. 20(1), 791 (2020). https://doi.org/10.1186/s12885-020-07256-8
11. M. A. Tomeh, R. Hadianamrei, X. Zhao.International journal of molecular sciences. 20(5), 1033 (2019). https://doi.org/10.3390/ijms20051033
12. M. Kundu, P. Sadhukhan, N. Ghosh, S. Chatterjee, P. Manna, J. Das, P. C. Sil.J Adv Res. 18, 161–172 (2019). https://doi.org/10.1016/j.jare.2019.02.036
13. S. J. Stohs, O. Chen, S. D. Ray, J. Ji, L. R. Bucci, H. G. Preuss. Molecules (Basel, Switzerland). 25(6), 1397 (2020). https://doi.org/10.3390/molecules25061397
14. M. Dei Cas, R. Ghidoni.Nutrients. 11(9), (2019). https://doi.org/10.3390/nu11092147
15. A. B. Kunnumakkara, C. Harsha, K. Banik, R. Vikkurthi, B. L. Sailo, D. Bordoloi, S. C. Gupta, B. B. Aggarwal.Expert Opin Drug Metab Toxicol. 15(9), 705–733 (2019). https://doi.org/10.1080/17425255.2019.1650914
16. W. P. T. D. Perera, R. K. Dissanayake, U. I. Ranatunga, N. M. Hettiarachchi, K. D. C. Perera, J. M. Unagolla, R. T. De Silva, L. R. Pahalagedara.RSC Advances. 10(51), 30785–30795 (2020). https://doi.org/10.1039/d0ra05755j
17. Z. Zeng, W. Zhang, D. M. Arvapalli, B. Bloom, A. Sheardy, T. Mabe, Y. Liu, Z. Ji, H. Chevva, D. H. Waldeck, J. Wei.Phys Chem Chem Phys. 19(30), 20101–20109 (2017). https://doi.org/10.1039/c7cp02875j
18. X. Gao, L. Wang, C. Sun, N. Zhou.Molecules (Basel, Switzerland). 27(5), 1690 (2022). https://doi.org/10.3390/molecules27051690
19. M. Behi, L. Gholami, S. Naficy, S. Palomba, F. Dehghani. Nanoscale Advances. 4(2), 353–376 (2022). https://doi.org/10.1039/D1NA00559F
20. J. Liu, R. Li, B. Yang.ACS Central Science. 6(12), 2179–2195 (2020). https://doi.org/10.1021/acscentsci.0c01306
21. M. Kinoshita, H. Kayama, T. Kusu, T. Yamaguchi, J. Kunisawa, H. Kiyono, S. Sakaguchi, K. Takeda.J Immunol. 189(6), 2869–2878 (2012). https://doi.org/10.4049/jimmunol.1200420
22. L. E. Kelemen. Int J Cancer. 119(2), 243–250 (2006). https://doi.org/10.1002/ijc.21712
23. S. H. Chen, T. I. Liu, C. L. Chuang, H. H. Chen, W. H. Chiang, H. C. Chiu.J Mater Chem B. 8(17), 3789–3800 (2020). https://doi.org/10.1039/d0tb00046a
24. N. Koirala, D. Das, E. Fayazzadeh, S. Sen, A. McClain, J. E. Puskas, J. A. Drazba, G. McLennan. J Biomed Mater Res A. 107(11), 2522–2535 (2019). https://doi.org/10.1002/jbm.a.36758
25. S. Nimmagadda, M. F. Penet.Front Oncol. 9, 1537 (2019). https://doi.org/10.3389/fonc.2019.01537
26. Y. Tie, H. Zheng, Z. He, J. Yang, B. Shao, L. Liu, M. Luo, X. Yuan, Y. Liu, X. Zhang, H. Li, M. Wu, X. Wei.Signal Transduct Target Ther. 5(1), 6 (2020). https://doi.org/10.1038/s41392-020-0115-0
27. S. Tan, G. Wang. Biomed Pharmacother. 102, 55–63 (2018). https://doi.org/10.1016/j.biopha.2018.03.046
28. W. Gao. in *Preparation and evaluation of folate receptor mediated targeting liposomes*. ed. by 2021), pp. 167–178
29. B. Frigerio, C. Bizzoni, G. Jansen, C. P. Leamon, G. J. Peters, P. S. Low, L. H. Matherly, M. Figini.Journal of experimental & clinical cancer research: CR. 38(1), 125 (2019). https://doi.org/10.1186/s13046-019-1123-1
30. D. J. Bharali, D. W. Lucey, H. Jayakumar, H. E. Pudavar, P. N. Prasad.Journal of the American Chemical Society. 127(32), 11364–11371 (2005). https://doi.org/10.1021/ja051455x
31. Z. Han, L. He, S. Pan, H. Liu, X. Hu.Luminescence. 35(7), 989–997 (2020). https://doi.org/10.1002/bio.3803
32. Z. A. B. Zakaria, M. A. M. Moklas, E. B. A. Rahim, S. M. Chiroma, A. Danmaigoro, K. Abubakar, M. M. Mailafiya.Biomedical Research and Therapy. 6(12), 3518–3540 (2019). https://doi.org/10.15419/bmrat.v6i12.580
33. Talevi, A., Ruiz, M.E. (2021). Korsmeyer-Peppas, Peppas-Sahlin, and Brazel-Peppas: Models of Drug Release. In: The ADME Encyclopedia. Springer, Cham. https://doi.org/10.1007/978-3-030-51519-5_35-1
34. S. M. Sreedharan, R. Singh. Int J Nanomedicine. 14, 9905–9916 (2019). https://doi.org/10.2147/IJN.S224488
35. S. Kadaikunnan, T. S. Rejiniemon, J. M. Khaled, N. S. Alharbi, R. Mothana.Annals of Clinical Microbiology and Antimicrobials. 14(1), 9 (2015). https://doi.org/10.1186/s12941-015-0069-1
36. N. Ghanbari, Z. Salehi, A. A. Khodadadi, M. A. Shokrgozar, A. A. Saboury. Mater Sci Eng C Mater Biol Appl. 121, 111809 (2021). https://doi.org/10.1016/j.msec.2020.111809
37. P. Skehan, R. Storeng, D. Scudiero, A. Monks, J. McMahon, D. Vistica, J. T. Warren, H. Bokesch, S. Kenney, M. R. Boyd.Journal of the National Cancer Institute. 82(13), 1107–1112 (1990). https://doi.org/10.1093/jnci/82.13.1107
38. K. Naik, S. Chaudhary, L. Ye, A. S. Parmar.Frontiers in Bioengineering and Biotechnology. 10, (2022). https://doi.org/10.3389/fbioe.2022.882100
39. X. Lin, M. Xiong, J. Zhang, C. He, X. Ma, H. Zhang, Y. Kuang, M. Yang, Q. Huang.Microchemical Journal. 160, (2021). https://doi.org/10.1016/j.microc.2020.105604
40. S. Kalytchuk, L. ZdraZil, M. Scheibe, R. Zboril.Nanoscale. 12(15), 8379–8384 (2020). https://doi.org/10.1039/d0nr00505c

41. Carbonaro, Corpino, Salis, Mocci, Thakkar, Olla, Ricci.C — Journal of Carbon Research. 5(4), (2019). https://doi.org/10.3390/c5040060
42. D. Tong, W. Li, Y. Zhao, L. Zhang, J. Zheng, T. Cai, S. Liu. RSC Advances. 6(99), 97137–97141 (2016). https://doi.org/10.1039/c6ra17068d
43. Y. Wang, X. Chang, N. Jing, Y. Zhang.Analytical Methods. 10(23), 2775–2784 (2018). https://doi.org/10.1039/c8ay00441b
44. X. Lin, Y. Cao, J. Li, D. Zheng, S. Lan, Y. Xue, F. Yu, M. Wu, X. Zhu.Biomater Sci. 7(7), 2996–3006 (2019). https://doi.org/10.1039/c9bm00276f
45. P. Manivasagan, S. W. Jun, V. T. Nguyen, N. T. P. Truong, G. Hoang, S. Mondal, M. Santha Moorthy, H. Kim, T. T. Vy Phan, V. H. M. Doan, C.-S. Kim, J. Oh. Journal of Materials Chemistry B. 7(24), 3811–3825 (2019). https://doi.org/10.1039/c8tb02823k
46. M. Z. Fahmi, N. F. Sholihah, A. Wibrianto, S. C. W. Sakti, F. Firdaus, J.-y. Chang.Materials Chemistry and Physics. 267, (2021). https://doi.org/10.1016/j.matchemphys.2021.124596
47. L. Shen, C. C. Liu, C. Y. An, H. F. Ji. Sci Rep. 6, 20872 (2016). https://doi.org/10.1038/srep20872
48. E. Faghfuri, M. Sagha, A. H. Faghfouri.Journal of Cluster Science. (2021). https://doi.org/10.1007/s10876-021-02125-1
49. W. Hong, F. Guo, N. Yu, S. Ying, B. Lou, J. Wu, Y. Gao, X. Ji, H. Wang, A. Li, G. Wang, G. Yang.Drug Des Devel Ther. 15, 2843–2855 (2021). https://doi.org/10.2147/DDDT.S320119
50. W. Y. Wang, Y. X. Cao, X. Zhou, B. Wei.Drug Des Devel Ther. 13, 2205–2213 (2019). https://doi.org/10.2147/DDDT.S205787
51. M. M. H. Khalil, H. Mahdy, D. Y. Sabry, E. H. Ismail. Journal of Scientific Research. 6(3), 509–519 (2014). https://doi.org/10.3329/jsr.v6i3.18750
52. K. Muthoosamy, I. B. Abubakar, R. G. Bai, H. S. Loh, S. Manickam.Sci Rep. 6(32808 (2016). https://doi.org/10.1038/srep32808
53. P. Yang, Z. Zhu, T. Zhang, W. Zhang, W. Chen, Y. Cao, M. Chen, X. Zhou. Small. 15(44), (2019). https://doi.org/10.1002/smll.201902823
54. V. J. Sawant, S. R. Bamane, D. G. Kanase, S. B. Patil, J. Ghosh.RSC Advances. 6(71), 66745–66755 (2016). https://doi.org/10.1039/c6ra13851a
55. S. Kazemi, M. Pourmadadi, F. Yazdian, A. Ghadami.Int J Biol Macromol. 186, 554–562 (2021). https://doi.org/10.1016/j.ijbiomac.2021.06.184
56. S. B. Ghaffari, M. H. Sarrafzadeh, Z. Fakhroueian, M. R. Khorramizadeh. Mater Sci Eng C Mater Biol Appl. 103, 109827 (2019). https://doi.org/10.1016/j.msec.2019.109827
57. M. Z. Fahmi, Y. Y. Aung, M. A. Ahmad, A. N. Kristanti, S. C. W. Sakti, O. P. Arjasa, H. V. Lee.Nanotheranostics. 7(3), 281–298 (2023). https://doi.org/10.7150/ntno.80030
58. M. Chen, L. Li, L. Xia, S. Jiang, Y. Kong, X. Chen, H. Wang. Carbohydr Polym. 265, 118077 (2021). https://doi.org/10.1016/j.carbpol.2021.118077
59. M. G. Montalban, J. M. Coburn, A. A. Lozano-Perez, J. L. Cenis, G. Villora, D. L. Kaplan. Nanomaterials (Basel). 8(2), (2018). https://doi.org/10.3390/nano8020126
60. M. M. Gottesman, T. Fojo, S. E. Bates.Nature Reviews Cancer. 2(1), 48–58 (2002). https://doi.org/10.1038/nrc706
61. X. Liang, J. Fan, Y. Zhao, M. Cheng, X. Wang, R. Jin, T. Sun. J. Biomaterials Applications. 31(9), 1247–1256 (2017). https://doi.org/10.1177/0885328217701289
62. S. Zhao, S. Sun, K. Jiang, Y. Wang, Y. Liu, S. Wu, Z. Li, Q. Shu, H. Lin. Nano-micro letters. 11(1), 32 (2019). https://doi.org/10.1007/s40820-019-0263-3
63. Z. Zhong, X. Li, S. Liu, C. Zhang, X. Xu, L. Liao.RSC Adv. 11(46), 28809–28817 (2021). https://doi.org/10.1039/d1ra04592j
64. C. Müller, R. Schibli.Journal of nuclear medicine: official publication, Society of Nuclear Medicine. 52(1), 1–4 (2011). https://doi.org/10.2967/jnumed.110.076018
65. G. L. Zwicke, G. A. Mansoori, C. J. Jeffery. Nano Rev. 3, https://doi.org/10.3402/nano.v3403i3400.18496 (2012). https://doi.org/10.3402/nano.v3i0.18496
66. Y. S. Yi.Immune Netw. 16(6), 337–343 (2016). https://doi.org/10.4110/in.2016.16.6.337
67. R. Zhao, N. Diop-Bove, M. Visentin, I. D. Goldman.Annu Rev Nutr. 31, 177–201 (2011). https://doi.org/10.1146/annurev-nutr-072610-145133
68. D. Jelovac, D. K. Armstrong.CA Cancer J Clin. 61(3), 183–203 (2011). https://doi.org/10.3322/caac.20113
69. C. Liu, L. Ding, L. Bai, X. Chen, H. Kang, L. Hou, J. Wang.Biochem Biophys Res Commun. 491(4), 1083–1091 (2017). https://doi.org/10.1016/j.bbrc.2017.08.015
70. H. Shi, J. Guo, C. Li, Z. Wang.Drug Des Devel Ther. 9, 4989–4996 (2015). https://doi.org/10.2147/DDDT.S90670
71. B. W. Blaser, M. Gonit, H. Qi, A. Shatnawi, M. Guimond, R. J. Lee, M. Ratnam.Leukemia. 21(10), 2233–2235 (2007). https://doi.org/10.1038/sj.leu.2404786
72. C. Chittasupho, A. Manthaisong, S. Okonogi, S. Tadtong, W. Samee.Int J Mol Sci. 23(1), (2021). https://doi.org/10.3390/ijms23010142
73. M. Jurczyk, K. Jelonek, M. Musial-Kulik, A. Beberok, D. Wrzesniok, J. Kasperczyk.Pharmaceutics. 13(3), (2021). https://doi.org/10.3390/pharmaceutics13030326
74. K. Vinothini, N. K. Rajendran, A. Ramu, N. Elumalai, M. Rajan.Biomed Pharmacother. 110, 906–917 (2019). https://doi.org/10.1016/j.biopha.2018.12.008
75. J. Pilch, P. Kowalik, A. Kowalczyk, P. Bujak, A. Kasprzak, E. Paluszkiewicz, E. Augustin, A. M. Nowicka. Int J Mol Sci. 23(3), (2022). https://doi.org/10.3390/ijms23031261
76. M. P. Shirani, B. Rezaei, T. Khayamian, M. Dinari, F. H. Shamili, M. Ramezani, M. Alibolandi.Materials science & engineering C, Materials for biological applications. 92, 892–901 (2018). https://doi.org/10.1016/j.msec.2018.07.043
77. H. S. Shang, C. H. Chang, Y. R. Chou, M. Y. Yeh, M. K. Au, H. F. Lu, Y. L. Chu, H. M. Chou, H. C. Chou, Y. L. Shih, J. G. Chung. Oncol Rep. 36(4), 2207–2215 (2016). https://doi.org/10.3892/or.2016.5002
78. A. Lewinska, J. Adamczyk, J. Pajak, S. Stoklosa, B. Kubis, P. Pastuszek, E. Slota, M. Wnuk.Mutat Res Genet Toxicol Environ Mutagen. 771, 43–52 (2014). https://doi.org/10.1016/j.mrgentox.2014.07.001
79. F. Ghasemi, M. Shafiee, Z. Banikazemi, M. H. Pourhanifeh, H. Khanbabaei, A. Shamshirian, S. Amiri Moghadam, R. ArefNezhad, A. Sahebkar, A. Avan, H. Mirzaei.Pathology, research and practice. 215(10), 152556 (2019). https://doi.org/10.1016/j.prp.2019.152556
80. W. Cai, B. Zhang, D. Duan, J. Wu, J. Fang.Toxicology and applied pharmacology. 262(3), 341–348 (2012). https://doi.org/10.1016/j.taap.2012.05.012
81. S. Pani, A. Sahoo, A. Patra, P. R. Debata.Biotechnology and applied biochemistry. 68(6), 1396–1402 (2021). https://doi.org/10.1002/bab.2061
82. G. Sethi, V. Tergaonkar.Trends Pharmacol Sci. 30(6), 313–321 (2009). https://doi.org/10.1016/j.tips.2009.03.004
83. A. B. Kunnumakkara, D. Bordoloi, G. Padmavathi, J. Monisha, N. K. Roy, S. Prasad, B. B. Aggarwal.Br J Pharmacol. 174(11), 1325–1348 (2017). https://doi.org/10.1111/bph.13621
84. J. M. Miller, J. K. Thompson, M. B. MacPherson, S. L. Beuschel, C. M. Westbom, M. Sayan, A. Shukla.Cancer Prev Res (Phila). 7(3), 330–340 (2014). https://doi.org/10.1158/1940-6207.CAPR-13-0259

85. S. Reuter, J. Charlet, T. Juncker, M. H. Teiten, M. Dicato, M. Diederich.Ann N Y Acad Sci. 1171, 436–447 (2009). https://doi.org/10.1111/j.1749-6632.2009.04731.x
86. M. Becit, A. Aydin Dilsiz, N. Basaran. Istanbul Journal of Pharmacy. 50(3), 202–210 (2020).
87. S.-Y. Teow, K. Liew, S. A. Ali, A. S.-B. Khoo, S.-C. Peh. J. Tropical Medicine. 2016, 2853045 (2016). https://doi.org/10.1155/2016/2853045
88. S. Mushtaq, T. Yasin, M. Saleem, T. Dai, M. A. Yameen. Photochem Photobiol. 98(1), 202–210 (2022). https://doi.org/10.1111/php.13503
89. S. H. Mun, D. K. Joung, Y. S. Kim, O. H. Kang, S. B. Kim, Y. S. Seo, Y. C. Kim, D. S. Lee, D. W. Shin, K. T. Kweon, D. Y. Kwon.Phytomedicine: international journal of phytotherapy and phytopharmacology. 20(8–9), 714–718 (2013). https://doi.org/10.1016/j.phymed.2013.02.006
90. P. Tyagi, M. Singh, H. Kumari, A. Kumari, K. Mukhopadhyay. PLoS One. 10(3), e0121313 (2015). https://doi.org/10.1371/journal.pone.0121313
91. S. Tajbakhsh, K. Mohammadi, I. Deilami, K. Zandi, M. Fouladvand, E. Ramedani, G. Asayesh.African Journal of Biotechnology. 7(21), (2008).
92. Bhawana, R. K. Basniwal, H. S. Buttar, V. K. Jain, N. Jain.Journal of Agricultural and Food Chemistry. 59(5), 2056–2061 (2011). https://doi.org/10.1021/jf104402t
93. K. Varaprasad, M. López, D. Núñez, T. Jayaramudu, E. R. Sadiku, C. Karthikeyan, P. Oyarzúnc.Journal of Molecular Liquids. 300, 112353 (2020). https://doi.org/10.1016/j.molliq.2019.112353
94. Y. Hussain, W. Alam, H. Ullah, M. Dacrema, M. Daglia, H. Khan, C. R. Arciola. Antibiotics. 11(3), 322 (2022).
95. G. Ramesh, J. E. Kaviyil, W. Paul, R. Sasi, R. Joseph. ACS omega. 7(8), 6795–6809 (2022). https://doi.org/10.1021/acsomega.1c06398
96. Z. Sadeghi-Ghadi, N. Behjou, P. Ebrahimnejad, M. Mahkam, H. R. Goli, M. Lam, A. Nokhodchi. J. Pharmaceutical Innovation (2022). https://doi.org/10.1007/s12247-022-09619-z